Observation of gravity-capillary wave turbulence

Eric Falcon, Claude Laroche, Stéphan Fauve

Observation of gravity-capillary wave turbulence

Éric Falcon,[1] Claude Laroche,[1] and Stéphan Fauve[2,*]

[1]*Laboratoire de Physique, École Normale Supérieure de Lyon, UMR 5672, 46, allée d'Italie, 69 007 Lyon, France*

[2]*Laboratoire de Physique Statistique, École Normale Supérieure, UMR 8550, 24, rue Lhomond, 75 005 Paris, France*

(Dated: submitted to Physical Review Letters the 7th of August 2006)

We report the observation of the cross-over between gravity and capillary wave turbulence on the surface of mercury. The probability density functions of the turbulent wave height are found to be asymmetric and thus non Gaussian. The surface wave height displays power-law spectra in both regimes. In the capillary region, the exponent is in fair agreement with weak turbulence theory. In the gravity region, it depends on the forcing parameters and is found in rough agreement with theory only for the largest forcing intensities. However, the scaling of those spectra with the mean energy flux is found in disagreement with weak turbulence theory for both regimes.

PACS numbers: 47.35.-i, 47.52.+j, 05.45.-a, 68.03.Cd

Wave turbulence, also known as weak turbulence, is observed in various situations: internal waves in the ocean [1], surface waves on a stormy sea [2], Alfvén waves in astrophysical plasmas [3], Langmuir waves [4] and ion waves [5] in plasmas, spin waves in solids. It has been also emphasized that wave turbulence should play an important role in nonlinear optics [6]. However, wave turbulence experiments are scarce compared to numerous studies on hydrodynamic turbulence. Most of them concern capillary or gravity waves. For short wavelengths, capillary wave turbulence has been observed by optical techniques [7–10]. It has been reported that the height of the surface displays a power-law frequency spectrum $f^{-17/6}$ in agreement with weak turbulence (WT) theory [11] and simulations [12]. For longer wavelengths, gravity wave turbulence has been mainly observed *in situ* (i.e. on the sea surface or in very large tanks) with wind-generated waves leading to power-law spectra f^{-4} [2] in agreement with isotropic WT theory [13] and simulations [14]. However, when the turbulence is not forced by wind or by an isotropic forcing, mechanisms of energy cascade in the inertial regime change, as well as the scaling law of the spectrum [14, 15], and are still a matter of debate.

Besides scalings with respect to frequency or wave number, Kolmogorov-type spectra also depend on the mean energy flux ϵ cascading from injection to dissipation. This dependence is related to the nature of nonlinear wave interactions which are different in capillary (3-wave interactions) versus gravity (4-wave interactions) regimes [11, 13]. To our knowledge, the mean energy flux has been never measured in wave turbulence and no experiment has been performed to study how spectra scale with ϵ. Matching the gravity and capillary spectra is another open question, since in the cross-over region, nonlinearities are not weak, and WT theory breaks down [16].

We report in this letter how power-law spectra in the gravity and capillary ranges depend on the forcing parameters of surface waves. We measure the mean energy flux ϵ and show that, although the scaling of the spectra with respect to frequency look in agreement with WT theory in some limits, their scaling on ϵ differ from theoretical predictions. We also observe that capillary and gravity spectra are matched together via a smooth cross-over region. The probability density distribution (PDF) of the turbulent wave-height is also measured and found to be non Gaussian.

The experimental setup consists of a quasi-rectangular plastic vessel, 20 cm side, filled with mercury up to a height, $h = 18$ mm. The properties of the fluid are, density, $\rho = 13.5\ 10^3$ kg/m^3, dynamic viscosity, $\mu = 1.5\ 10^{-3}$ Ns/m^2 and surface tension $\gamma = 0.4$ N/m. The choice of mercury has been motivated by its low kinematic viscosity which is an order of magnitude smaller than that of water, thus strongly reducing wave dissipation. Contrarily to the usual bulk excitation of waves by Faraday vibrations [7, 8], surface waves are generated by the horizontal motion of two rectangular (10×3.5 cm^2) plunging PMMA wave makers driven by two electromagnetic vibration exciters (BK 4809) via a power supplied (Kepco Bop50-4A). The wave makers are driven with random noise excitation, supplied by a function generator (SR-DS345), and selected in a frequency range 0 - f_{driv} with $f_{driv} = 4$ to 6 Hz by a low-pass filter (SR 640). This is in contrast with most previous experiments on capillary wave turbulence driven by one excitation frequency [7, 8, 10]. Surface waves are generated 2.2 cm inward from two adjacent vessel walls and the local displacement of the fluid in response to these excitations is measured 7 cm away from the wave makers. A capacitive wire gauge, perpendicular to the fluid surface at rest, is made of an insulated copper wire, 0.1 mm in diameter. The insulation (a varnish) is then the dielectric of an annular capacitor with the wire as the inner conductor and mercury as the outer one. The capacitance is thus proportional to the

fluid level. A low-cost home-made analogic multivibrator with a response time 0.1 ms is used as a capacitance meter in the range 0 – 200 pF. The linear sensing range of the sensor allows wave height measurements from 10 μm up to 2 cm with a 20 mm/V sensitivity. Although resistance or capacitance wire probes are widely used to get precise measurements of the level of quasi-static liquids, their dynamical response in the case of a rapidly varying wavy surface is not well known due to possible meniscus effects [17, 18]. Thus, we have first checked our results with measurements performed with eddy current displacement transducers or with an optical determination of the local slope of the surface [19]. The computation of the surface elevation from the optical signal has been found in good agreement with the direct capacitive measurement of sinusoidal wave amplitude in the frequency range up to 150 Hz. Although the sensitivity, the response time and the spatial resolution of the optical technique are better, the capacitive method allows a direct measurement of the surface displacement in a wide amplitude range and does not require signal processing. Besides simplicity, this gives also more accurate measurements of complex wave shapes because small errors may accumulate due to the numerical integration necessary to process the optical signal.

The mean energy flux injected by the wave makers and dissipated by viscosity is determined as follows. The velocity $V(t)$ of the wave maker is measured using a coil placed on the top of the vibration exciter. The *e.m.f.* generated by the moving permanent magnet of the vibration exciter is proportional to the excitation velocity. The force $F(t)$ applied by the vibration exciter to the wave maker is measured by a piezoresistive force transducer (FGP 10 daN). The power injected into the fluid by the wave maker is $I(t) = -F_R(t)V(t)$ where $F_R(t)$ is the force applied by the fluid on the wave maker. It generally differs from $F(t)V(t)$ which is measured here but their time averages are equal, thus $\langle I \rangle = \langle F(t)V(t) \rangle$.

A typical recording of the surface wave amplitude at a given location is displayed in Fig. 1 as a function of time. The wave amplitude is very erratic with a large distribution of amplitudes. The largest values of the amplitude are of the order of the depth of fluid at rest, whereas the mean value of the amplitude is close to zero.

The probability density function (PDF) of the surface wave height, η, at a given location is displayed in Fig. 2 for various forcing intensities. For a given excitation band width, the *rms* value, σ_V, of the velocity fluctuations of the wave maker is proportional to the driving voltage U_{rms} applied to the vibration exciter. At low forcing, the statistical distribution of wave heights is Gaussian, whereas at high enough forcing the PDF becomes asymmetric. The positive rare events such as high crest waves are more probable than deep trough waves. This can also be directly observed on the temporal signal $\eta(t)$ in Fig. 1. A similar asymetrical distribution is observed when using water instead of mercury, although the meniscus has an opposite concavity. Thus the asymmetry does not result from a dynamical effect of meniscus hysteresis [18]. This asymmetry increases with the forcing amplitude, whereas the mean value $\langle \eta \rangle$ remains close to zero as shown by the PDFs of the reduced variable $\eta/\langle \eta^2 \rangle^{1/2}$. A more quantitative estimate can be obtained by looking at the skewness $S \equiv \langle \eta^3 \rangle / \langle \eta^2 \rangle^{3/2}$ and the flatness $F \equiv \langle \eta^4 \rangle / \langle \eta^2 \rangle^2$ of the PDFs. When the forcing increases, S increases from 0 (the Gaussian value) to 0.7 whatever the driving frequency, whereas F remains close to 3 (the Gaussian value) for 0 – 6

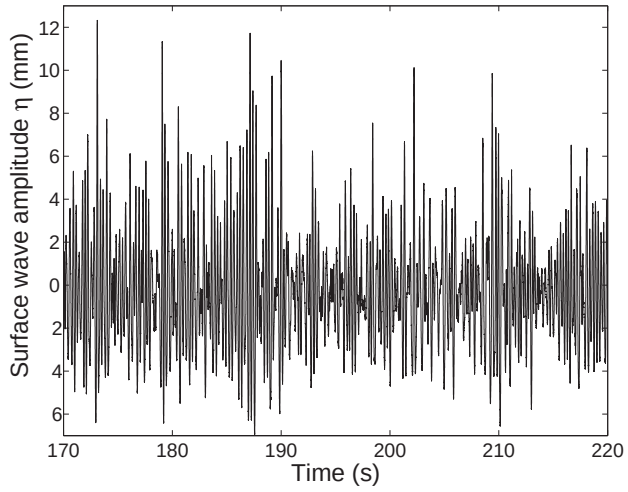

FIG. 1: Time recording of the surface wave height, $\eta(t)$, at a given location during 50 s. $\langle \eta \rangle \simeq 0$.

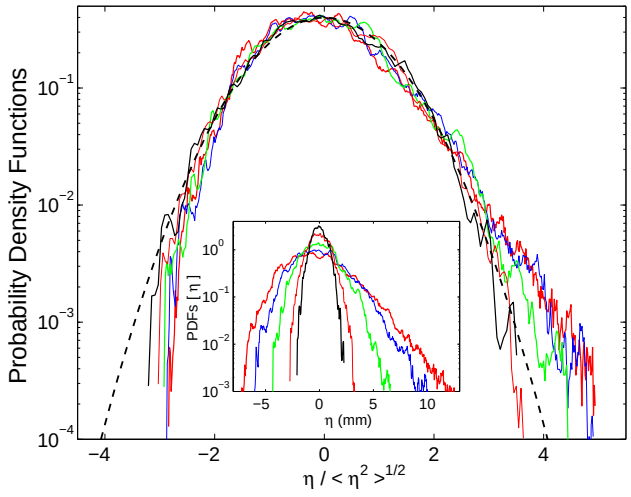

FIG. 2: Inset: Probability density functions of the wave-height, η, for 5 different values of the forcing amplitude, U_{rms} = 0.2, 0.3, 0.5, 0.7 and 0.9 V. The frequency band is $0 \leq f \leq 4$ Hz. Main: Same PDFs displayed using the reduced variable $\eta/\sqrt{\langle \eta^2 \rangle}$. Gaussian fit with zero mean and unit standard deviation (−−).

Hz, and slightly increases from 3 to 4 for 0 – 4 Hz driving.

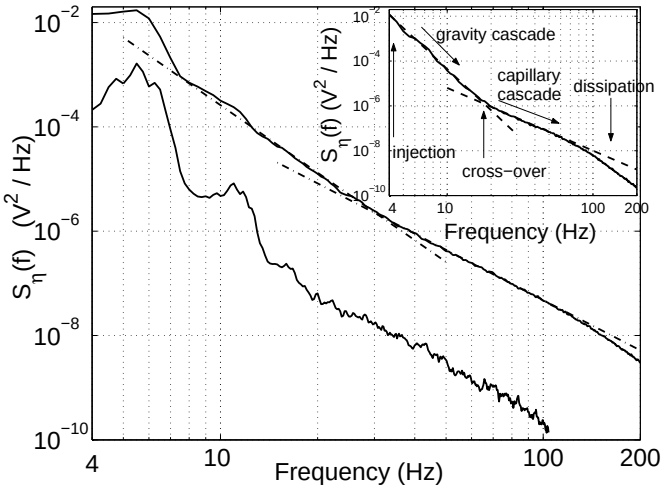

FIG. 3: Power spectra of the surface wave height for two different driving voltages $U_{rms} = 0.2$ and 0.9 V (from bottom to top). The frequency band is $0 \leq f \leq 6$ Hz. Dashed lines have slopes -4.3 and -3.2. Inset: The frequency band is $0 \leq f \leq 4$ Hz, and $U_{rms} = 0.9$ V. Dashed lines had slopes of -6.1 and -2.8.

The power spectrum $S_\eta(f)$ of the surface wave amplitude is recorded from 4 Hz up to 200 Hz and averaged during 2000 s. For small forcing, peaks related to the forcing and its harmonic are visible in the low frequency part of the spectrum in Fig. 3. At higher forcing, those peaks are smeared out and a power-law can be fitted. At higher frequencies, the slope of the scale invariant spectrum changes, and a cross-over is observed near 30 Hz between two regimes. This corresponds to the transition from gravity to capillary wave turbulence. At still higher frequencies (greater than 150 Hz), viscous dissipation dominates and ends the energy cascade. For a narrower frequency band of excitation (0 - 4 Hz), similar spectra are found but with a broader power-law in the gravity range (see inset of Fig. 3). When the two wave makers are driven with two noises with different band widths, *e.g.* 0 - 4 Hz and 0 - 6 Hz, the harmonic peak is no longer present, and gravity spectra display a power-law even at low driving amplitude.

For linear waves, the cross-over between gravity and capillary regimes corresponds to a wave number k of the order of the inverse of the capillary length $l_c \equiv \sqrt{\gamma/(\rho g)}$, *i.e.* to a critical frequency, $f_c = \sqrt{g/2l_c}/\pi$, where g is the acceleration of gravity. For mercury, $l_c = 1.74$ mm and $f_c \simeq 17$ Hz corresponding to a wavelength of the order of 1 cm. The insets of Fig. 3 and Fig. 4 show a correct agreement in the case of a narrow driving frequency band. We also observe that the cross-over frequency increases with the driving amplitude and with the width of the driving frequency band. This may be due to the fact that the above estimate of f_c is only valid for linear waves.

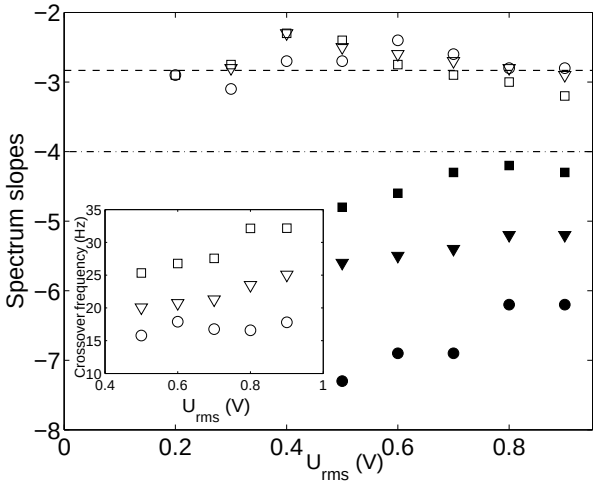

FIG. 4: Slopes of surface-height spectra for gravity (full symbols) and capillary (open symbols) waves for different forcing band widths and intensities: (○) 0 to 4 Hz, (▽) 0 to 5 Hz and (□) 0 to 6 Hz. Power-law exponents of gravity wave spectrum ($-\cdot$) and capillary waves spectrum ($--$) as predicted by WT theory (Eq. 1). Inset: Cross-over frequency between gravity and capillary regimes as a function of the forcing intensity and band width.

Surface wave turbulence is usually described as N interacting waves governed by kinetic-like equations in case of small nonlinearity and weak wave interactions. WT theory predicts that the surface height spectrum is scale invariant with a power-law frequency dependence. Such a Kolmogorov-like spectrum writes

$$\begin{aligned} &S_\eta(f) \propto \epsilon^{\frac{1}{2}} \left(\frac{\gamma}{\rho}\right)^{\frac{1}{6}} f^{-\frac{17}{6}} \text{ for capillary waves [11],} \\ &S_\eta(f) \propto \epsilon^{\frac{1}{3}} g f^{-4} \text{ for gravity waves [13],} \end{aligned} \quad (1)$$

where ϵ is the energy flux per unit surface and density. In both regimes, these frequency power-law exponents are compared in Fig. 4 with the slopes of surface height spectra measured for different forcing intensities and band widths. The experimental values of the scaling exponent of capillary spectra are close to the expected $f^{-2.8}$ scaling as already shown with one driving frequency [7, 8, 10] or with noise [10]. Figure 4 shows that this exponent does not depend on the amplitude and the frequency band of the forcing, within our experimental precision. For the gravity spectrum, no power-law is observed at small forcing since turbulence is not strong enough to hide the first harmonic of the forcing (see Fig. 3). At high enough forcing, the scaling exponent of gravity spectra is found to increase with the intensity and the frequency band (see Fig. 4). For gravity waves, the predicted f^{-4} scaling of Eq. (1) is only observed for the largest forcing intensities and band width (see Fig. 4).

We finally consider how those spectra scale with the mean energy flux ϵ per unit surface and density, defined by $\epsilon = \langle I \rangle / \rho S$ where $\langle I \rangle$ is the mean power injected by the wave maker and S is the area of the mercury layer. Using dimensional arguments, we obtain $\epsilon = (\gamma g/\rho)^{3/4} F(g\gamma/\rho\sigma_V^4)$ where F is some arbitrary function. Our measurements show $\langle I \rangle \propto \sigma_V^2$ with a proportionality coefficient of order 10 W/(m/s)^2. Then, we obtain $\epsilon \propto (g\gamma/\rho)^{1/4}\sigma_V^2$ with a proportionality constant of order 0.15. We note that the largest values of ϵ are more than one order of magnitude smaller than the critical flux $(\gamma g/\rho)^{3/4} \approx 2200$ (cm/s)^3) corresponding to the breakdown of weak turbulence [16].

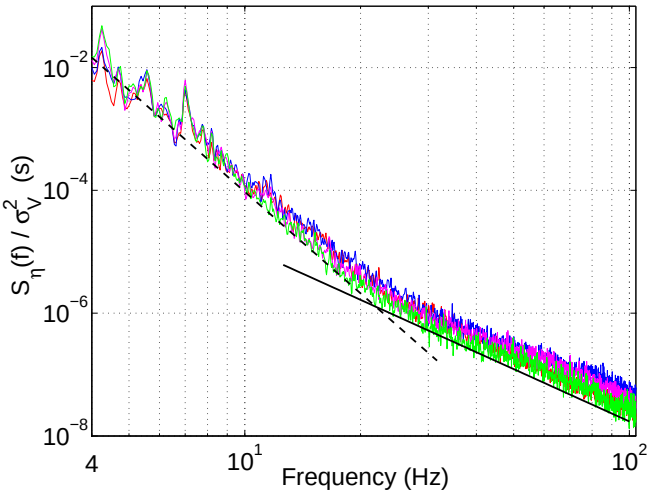

FIG. 5: Spectra of the surface wave amplitude divided by the variance σ_V^2 of the velocity of the wave maker for different forcing amplitudes, $\sigma_V = 2.1, 2.6, 3.5$ and 4.1 cm/s. The frequency band is $0 \leq f \leq 4$ Hz. The dashed line has slope -5.5 whereas the full line has slope $-17/6$.

Dimensional arguments in the case of pure capillary (respectively gravity) regimes, give

$$\begin{aligned} S_\eta(f) &\propto \frac{(\gamma/\rho)^3}{\sigma_V^7}\, G\left(\frac{\gamma f}{\rho\sigma_V^3}\right) \text{ for capillary waves} \\ S_\eta(f) &\propto \frac{\sigma_V^5}{g^3}\, H\left(\frac{\sigma_V f}{g}\right) \text{ for gravity waves} \end{aligned} \qquad (2)$$

where G and F are arbitrary functions. In those limits, a power-law dependence of the spectrum on f thus implies a corresponding power-law dependence on σ_V or on ϵ. The best choice in order to collapse our experimental spectra on a single curve for different values of σ_V is displayed in Fig. 5 where $S_\eta(f)/\sigma_V^2$ is plotted versus f. Surprisingly, spectra are collapsed on both the gravity and capillary ranges by this single scaling. Their dependence on the mean energy flux ϵ thus correspond neither to prediction of WT theory for the capillary regime ($\epsilon^{1/2}$) nor to the one related to the gravity regime ($\epsilon^{1/3}$). This discrepancy can result from several reasons. First, the size of the container is too small to reach a forcing-independent gravity regime. Second, capillary and gravity regimes probably interact such that it may be wrong to consider them independently as in dimensional arguments leading to Eq. (2). Third, we observed that the energy flux strongly fluctuates and takes both positive and negative instantaneous values much larger than its mean [20]. The possible effect of these fluctuations on wave turbulence deserves further studies.

We thank F. Palierne for his help and B. Castaing, L. Biven and A. Newell for fruitful discussions. This work has been supported by the French Ministry of Research under Grant ACI 2001 and by the CNES.

* Corresponding author. Email address: fauve@lps.ens.fr

[1] Y. V. Lvov, K. L. Polzin and E. G. Tabak, Phys. Rev. Lett. **92**, 128501 (2004).
[2] Y. Toba, J. Ocean Soc. Jpn. **29**, 209 (1973); K. K. Kahma, J. Phys. Oceanogr. **11**, 1503 (1981); G. Z. Forristall, J. Geophys. Res. **86**, 8075 (1981); M. A. Donelan et al., Philos. Trans. R. Soc. London A **315**, 509 (1985).
[3] R. Z. Sagdeev, Rev. Mod. Phys. **51**, 1 (1979).
[4] J. D. Huba, P. K. Chaturvedi and K. Papadopoulos, Phys. Fluids **23**, 1479 (1980); M. Y. Yu and P. K. Shukla, Phys. Fluids **25**, 573 (1982).
[5] K. Mizuno and J. S. DeGroot, Phys. Fluids **26**, 608 (1983).
[6] E. Kuznetsov, A. C. Newell and V. E. Zakharov, Phys. Rev. Lett. **67**, 3243 (1991).
[7] W. B. Wright, R. Budakian and S. J. Putterman, Phys. Rev. Lett. **76**, 4528 (1996); W. B. Wright, R. Budakian, D. J. Pine and S. J. Putterman, Science **278**, 1609 (1997).
[8] M. Lommer and M. T. Levinsen J. Fluoresc. **12**, 45 (2002); E. Henry, P. Alstrøm and M. T. Levinsen, Europhys. Lett. **52**, 27 (2000).
[9] R. G. Holt and E. H. Trinh, Phys. Rev. Lett. **77**, 1274 (1996).
[10] M. Yu. Brazhinikov, G. V. Kolmakov and A. A. Levchenko, Sov. Phys JETP **95**, 447 (2002); M. Yu. Brazhinikov et al., Europhys. Lett. **58**, 510 (2002); G. V. Kolmakov et al. Phys. Rev. Lett. **93**, 074501 (2004).
[11] V. E. Zakharov and N. N. Filonenko, J. App. Mech. Tech. Phys. **8**, 37 (1967).
[12] A. N. Pushkarev and V. E. Zakharov, Phys. Rev. Lett. **76** 3320 (1996).
[13] V. E. Zakharov and N. N. Filonenko, Sov. Phys. Dokl. **11**, 881 (1967); V. E. Zakharov and M. M. Zaslavsky, Izv. Atm. Ocean. Phys. **18**, 747 (1982).
[14] M. Onorato et al., Phys. Rev. Lett. **89**, 144501 (2002); A. Pushkarev, D. Resio and V. Zakharov, Physica D **184** 29 (2003); A. I. Dyachenko, A. O. Korotkevich and V. E. Zakharov, Phys. Rev. Lett. **92**, 134501 (2004).
[15] S. A. Kitaigorodskii, J. Phys. Oceanogr. **13**, 816 (1983).
[16] C. Connaughton, S. Nazarenko and A. C. Newell, Physica D **184** 86 (2003).
[17] P. A. Lange et al., Rev. Sci. Instrum. **51**, 651 (1982).
[18] D. Quéré and A. de Ryck, Ann. Phys. Fr., **23** 1 (1998), in french.
[19] E. Falcon, C. Laroche and S. Fauve, Phys. Rev. Lett. **89**,

204501 (2002); Phys. Rev. Lett. 91, 064502, (2003).
[20] E. Falcon, C. Laroche and S. Fauve, "Fluctuations of energy flux in wave turbulence", in preparation (2006).